Hindawi
International Journal of Antennas and Propagation
Volume 2019, Article ID 1485075, 8 pages
https://doi.org/10.1155/2019/1485075

Research Article

Optimization of Sparse Concentric Ring Arrays for Low Sidelobe

Kesong Chen, Yafei Li, and Jiajia Shi

School of Information and Communication Engineering, University of Electronic Science and Technology of China, Chengdu 611731, China

Correspondence should be addressed to Yafei Li; li1367356@163.com

Received 22 January 2019; Accepted 30 April 2019; Published 2 June 2019

Academic Editor: Xiulong Bao

To lower the peak sidelobe level (PSLL) of sparse concentric ring arrays, a method with multiple design constraints that embed a function model into modified real genetic algorithm (MGA) and select the grid ring radii as optimization individual to synthesize sparse concentric ring arrays is proposed. The multiple constraints include the array aperture, the minimum element spacing, and the number of elements. The proposed method dynamically calculates the ratio of element on each ring, and it has a faster convergence rate than other algorithms. The MGA uses real number to code the optimization variable, and it reduces the complexity of coding and improves the search efficiency. Finally, the results demonstrate the accuracy and effectiveness of the algorithm.

1. Introduction

Antenna array plays an important role in technology, including mobile communication, radar system, satellite, and medical treatment. For example, in [1], a concentric ring array antenna is designed for reconfigurable isoflux pattern, which uses 61 elements, and the frequency is 2.8 GHz. The antenna arrays can reduce the volume occupation and complex feeding and heat dissipation systems in a satellite antenna system. In [2], a sparse concentric rings array with isoflux coverage to earth surface is designed for low earth orbit (LEO) satellite system, which optimizes the angular separation between the antenna elements and the amplitude excitation across the array to generate the characteristics of the desired isoflux radiation. The proposed antenna arrays can generate a wide isoflux pattern with a good accuracy with respect to the isoflux mask for LEO satellites. In [3], a repeater antenna is designed for wireless body area networks (WBAN) applications, which can obtain the biological information by implanting the device to human-body for treatment, diagnosis, and potential medical applications.

The PSLL is an important criterion to evaluate the performance of the antenna array. Thus, with the multiple design constraints, including the number of elements, the aperture of array, and the minimum spacing of element, it is an important research topic to reduce the PSLL of antenna array in recent years [4]. Study on array synthesis had been carried out for many years and produced many classical methods. These methodologies include Woodward Lawson method and optimization calculation method [5, 6], which can be used to improve pattern performance, and Taylor synthesis method [7], which can be applied to obtain a given pattern. With the development of array antenna, the scale of arrays becomes larger and the structure of arrays becomes complex; the traditional method of array synthesis is no longer applicable. So a lot of intelligence methods were introduced to synthesize array antenna, including genetic algorithm (GA), simulated annealing algorithm (SAA), differential evolution algorithm (DEA), and particle swarm optimization (PSO) [8–11]. There are a few other topics about circular antenna arrays, such as the design of nonuniform circular antenna arrays for low sidelobe [12, 13], the comparison of algorithms about the multiobject design of circular antenna arrays [14], the design of electronically steerable linear arrays [15], and the synthesis of sparse circular antenna arrays for acquiring desired radiation beam pattern [16]. This article selects GA to synthesize the sparse concentric ring arrays for low PSLL. In [17], GA was proposed. In [8], GA was applied to optimize thinned array antenna and acquired efficient result. In [18], a modified real genetic algorithm (MGA) was proposed to synthesize the sparse concentric ring arrays.

Due to the difference of element sparsity degree on each auxiliary ring [19], a function model that presents the

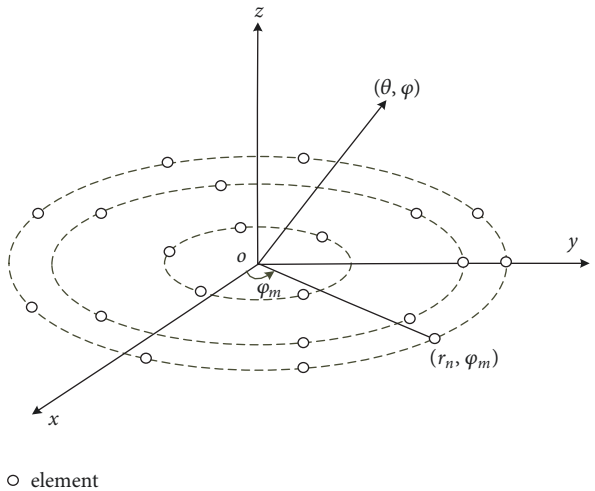

Figure 1: Diagram of concentric ring array.

relationship between ring radius and the degree of sparsity is proposed in this paper, which is embedded into the process of MGA to synthesize the sparse concentric ring arrays for low PSLL. The proposed method dynamically calculates the ratio of element on each ring, so it has a faster convergence rate than other algorithms. Besides, the MGA uses real number to code the optimization variable, and it reduces the complexity of coding and improves the search efficiency. Comparing the result to that of other algorithms, the proposed method can reduce PSLL efficiently and has a faster convergence.

2. The Optimization Model of Sparse Concentric Ring Array

In a planar array, generate a point randomly; the point is selected as centre point, and then generate several circles with different radius and place some elements on each ring; the resulting planar array is a concentric ring array [20]. The diagram of concentric ring array is shown in Figure 1.

Place an element in the centre of the concentric ring array; the radiation pattern can be described as

$$F(\mathrm{u}, v) = 1 + \sum_{n=1}^{H} \omega_n \sum_{m=1}^{N_\mathrm{n}} \exp\left[jkr_n\left(\cos\varphi_m u + \sin\varphi_m v\right)\right] \quad (1)$$

where

N_n = number of elements in ring n
H = number of rings
$k = 2\pi/\lambda$
λ = wavelength
ω_n = element weights for ring n
r_n = radius for ring n
$(r_n \cos\varphi_m, r_n \sin\varphi_m)$ = element location
$u = \sin\theta\cos\varphi$; $v = \sin\theta\sin\varphi$
$\varphi_m = 2\pi(m-1)/N_n$

For simplicity, we assume that array antenna meets the ideal conditions, including the element that is isotropic and the element that has uniform excitation amplitude and phase shift. The weight in the same ring is equal, and the elements in each ring are uniform distribution. The direction of main beam of the array points to the normal direction of the array, and the array pattern can be described as

$$F(\mathrm{u}, v) = 1 + \sum_{\mathrm{i}=1}^{N-1} \omega_\mathrm{i} \exp\left[jk\left(r_i \cos\varphi_i u + r_i \sin\varphi_i v\right)\right] \quad (2)$$

where N is the sum of element number, r_i is the radius of ith element, and φ_i is the angle of ith element.

If the sparse concentric ring array has multiple constraints, including the number of rings H, the maximum array aperture L, the minimum element spacing d_c, and the number of elements N, the optimization goal is to obtain the minimum PSLL, and the optimal mathematical model can be described as

$$\begin{gathered} \min\left\{PSLL\left(\mathrm{r}_0, r_1, \ldots, r_n, \ldots, r_H\right)\right\} \\ N_n = \left\lfloor \frac{2\pi r_n}{d_n} \right\rfloor, \quad 0 < d_c < d_n, \ n = 1, 2, \ldots, H \\ \sum_{n=0}^{H} N_n = N \end{gathered} \quad (3)$$

where

$$PSLL\left(r_0, r_1, \ldots, r_n, \ldots, r_H\right) = \max\left\{\left|\frac{F(u, v)}{FF_{\max}}\right|\right\} \quad (4)$$

where FF_{max} is the maximum value of array pattern; u, v are the regions excluding the main beam; N_n is the element number of nth rings. Due to the fact that the elements number of each ring must be an integer, the value of N_n must be rounded up or down to an integer. To meet the requirement of minimum element spacing $d_n \geq d_c$, the digits to the right of the decimal point are discarded.

3. The Algorithm of Optimization

The flowchart of function model algorithm using MGA is shown in Figure 2.

3.1. Function Model. There is a conclusion in [19]: in the sparse concentric ring array, when the ring is away from the array centre, the more sparsity the element is, the lower the PSLL is. Thus we can propose a function model to present the relation between ring radius and the degree of sparsity. We select the data of [21] as fitting data shown in Table 1.

In Table 1, N_n is the actual element number of nth rings, and N_{nmax} is the maximum element number nth ring can place.

$$N_{\mathrm{nmax}} = \left\lfloor \frac{2\pi r_n(\lambda)}{d_\mathrm{c}} \right\rfloor \quad (5)$$

P_n is element retention rate of nth ring.

$$P_n = \frac{N_n}{N_{\mathrm{nmax}}} \quad (6)$$

Table 1: The fitting data: element number (N), ring radii ($r_n(\lambda)$), actual element number in the rings (N_n), maximum element number (N_{nmax}), and element retention rate (P_n).

method	PSLL (dB)	N	n	1	2	3	4	5	6
Opt r_n&N_n [16]	-27.82	142	$r_n(\lambda)$	0.76	1.36	2.09	2.99	3.78	4.70
			N_n	9	17	25	31	26	33
	N_{nmax}			9	17	26	37	47	59
	P_n			9/9	16/16	25/26	31/37	26/47	33/59

Table 2: The function model fits the data in Table 1.

Function model	Model parameter			
	a	b	c	R^2
Linear model: $f(x) = a(\sin(x-\pi)) + b((x-10)^2) + c$	-0.1969	0.00228	0.6543	0.9602
Gauss model: $f(x) = a \cdot \exp(-((x-b)/c)^2)$	1.015	0.716	4.705	0.9168
Sine model: $f(x) = a \cdot \sin(b \cdot x + c)$	1.054	0.2152	1.633	0.9018
Power model: $f(x) = a \cdot x^b$	1.013	-0.2878		0.6812
Rational model: $f(x) = a/(x+b)$	5.468	4.315		0.7541
Polynomial model: $f(x) = a \cdot x + b$	-0.1331	1.166		0.8791

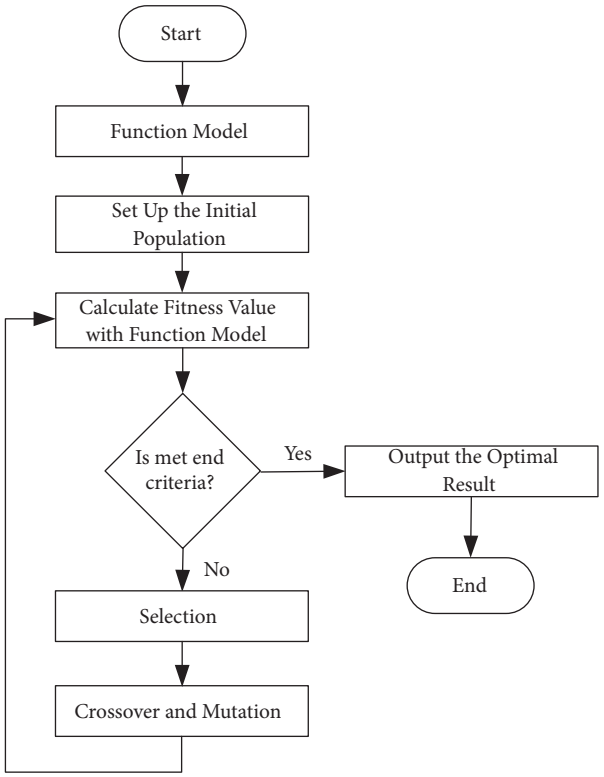

Figure 2: The flowchart of function model algorithm using MGA.

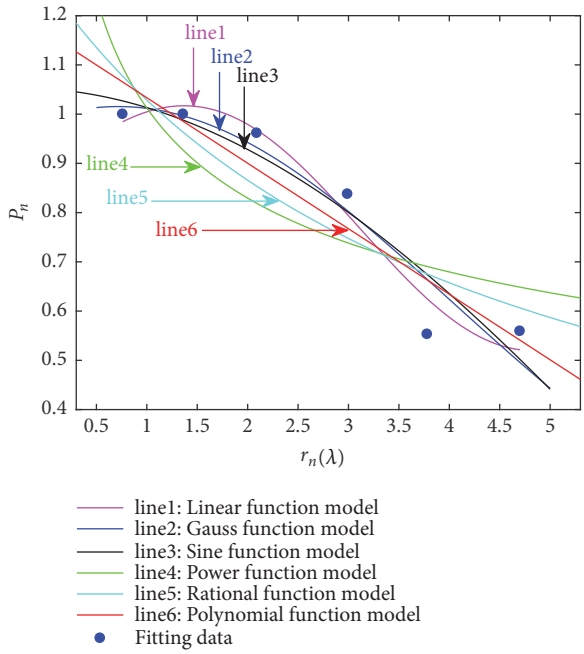

Figure 3: Function model diagram.

Different function model is used to fit the data of Table 1, and the result is shown in Table 2.

Plot the fitting data and function model in Figure 3.

In the fitting function model, the R^2 is the determination coefficient of fitting degree, and the larger the R^2 is, the higher the fitting degree is. In Table 2, the linear model has the maximum R^2, so the linear model is selected as fitting function model.

$$F(X) = a(\sin(X-\pi)) + b\left((X-10)^2\right) + c \quad (7)$$

X is the radius of circular; the value of $F(X)$ is the retention rate of ring with radius X. a, b, c are the coefficients of the function model, and they will be different with the variety of the number of elements and the size of the rings. The actual element number of rings with radii r_n can be calculated as follows:

$$N_n = \left\lfloor F(r_n) \cdot \left(\frac{2\pi r_n}{d_c}\right) \right\rfloor \quad (8)$$

3.2. The Process of MGA. Standard genetic algorithm uses 0,1 binary code for individual, and it has a low efficiency. MGA uses real number code for individual directly, and it has a high freedom of search and efficiency. The main steps of MGA include generating initial population, calculating fitness value, selection, crossover, and mutation.

3.2.1. Set Up the Initial Population. We select ring radii $\boldsymbol{R} = [r_0, r_1, r_2, \ldots, r_n, \ldots, r_H]$ as optimization individual. In order to meet the requirement of minimum element space d_c, an increasing function is used to generate the ring radius as follows:

$$\begin{aligned} r_n &= r_{n-1} + d_c + a \cdot n \quad a > 0 \\ r_0 &= 0, \\ r_{\mathrm{H}} &= \frac{L}{2} \end{aligned} \tag{9}$$

Generate individual repeatedly to make up the population $\boldsymbol{P}$.

$$\boldsymbol{P} = [\boldsymbol{R}_1, \boldsymbol{R}_2, \ldots, \boldsymbol{R}_k] \tag{10}$$

k is the individual number of the population $\boldsymbol{P}$.

3.2.2. Calculate Fitness Value with Function Model. Bring $\boldsymbol{R}$ into equation (5), so the maximum element number of each ring can be calculated. Equation (7) can calculate the retention rate of each ring; thus the actual element number in each ring can be acquired. Because the element in each ring is uniform distribution, the angle of mth element on the nth ring can be calculated as follows:

$$\varphi_m = \frac{2\pi\,(m-1)}{N_n} \quad 1 < m < N_n \tag{11}$$

The polar coordinate representation of the individual is as follows:

$$\boldsymbol{R}_c = \begin{bmatrix} r_1 + 0j & r_1 + 2\pi j\dfrac{2}{N_1} & \cdots & r_1 + 2\pi j\dfrac{N_1 - 1}{N_1} \\ \cdots & \cdots & \cdots & \cdots \\ r_n + 0j & r_n + 2\pi j\dfrac{2}{N_n} & \cdots & r_n + 2\pi j\dfrac{N_n - 1}{N_n} \\ \cdots & \cdots & \cdots & \cdots \\ r_H + 0j & r_H + 2\pi j\dfrac{2}{N_H} & \cdots & r_H + 2\pi j\dfrac{N_H - 1}{N_H} \end{bmatrix} \tag{12}$$

Substitute $\boldsymbol{R}_c$ into equation (4), so the fitness value can be calculated.

3.2.3. Judgement of Termination Condition. If the termination conditions (the number of iterations reaches the limit or the PSLL meets the requirement) are met, output the optimal individual and the minimum PSLL of the current population, end. Otherwise, continue.

3.2.4. Selection Operation. Sort the individual according to fitness value.

$$\boldsymbol{P}_s = sort\,[\boldsymbol{R}_1, \boldsymbol{R}_2, \ldots, \boldsymbol{R}_k] = [\boldsymbol{R}_{s1}, \boldsymbol{R}_{s2}, \ldots, \boldsymbol{R}_{sk}] \tag{13}$$

Select the excellent individual by mean of truncated selection rate p_t.

$$\boldsymbol{P}_E = \left[\boldsymbol{R}_{s1}, \boldsymbol{R}_{s2}, \ldots, \boldsymbol{R}_{s(\lfloor k \cdot p_t \rfloor)}\right] \tag{14}$$

Replicate $\boldsymbol{P}_E$ to make up new population $\boldsymbol{P}_{new}$ as genetic operator.

$$\begin{aligned} \boldsymbol{P}_{new} = [\boldsymbol{P}_E, \boldsymbol{P}_E, \ldots] = \big[&\boldsymbol{R}_{s1}, \boldsymbol{R}_{s2}, \ldots, \boldsymbol{R}_{s(\lfloor k \cdot p_t \rfloor)}, \boldsymbol{R}_{s1}, \boldsymbol{R}_{s2}, \\ &\ldots, \boldsymbol{R}_{s(\lfloor k \cdot p_t \rfloor)}, \ldots, \boldsymbol{R}_{s(k - \lfloor k/\lfloor k \cdot p_t \rfloor \rfloor \cdot \lfloor k \cdot p_t \rfloor)}\big] \end{aligned} \tag{15}$$

The number of individuals in $\boldsymbol{P}_{new}$ is equal to k.

3.2.5. Crossover and Mutation. In order to meet the requirement of minimum element spacing d_c, we need to set some constraints in process of crossover and mutation.

Crossover. If the nth genes of ith and jth individuals are selected as crossover gene.

The precrossover genetic operator is

$$\begin{aligned} \boldsymbol{R}_i &= [r_{i0}, r_{i1}, r_{i2}, \ldots, r_{in}, \ldots, r_{iH}] \\ \boldsymbol{R}_j &= \left[r_{j0}, r_{j1}, r_{j2}, \ldots, r_{jn}, \ldots, r_{jH}\right] \end{aligned} \tag{16}$$

The postcrossover genetic operator is

$$\begin{aligned} \boldsymbol{R}_i' &= \left[r_{i0}, r_{i1}, r_{i2}, \ldots, r_{jn}, \ldots, r_{iH}\right] \\ \boldsymbol{R}_j' &= \left[r_{j0}, r_{j1}, r_{j2}, \ldots, r_{in}, \ldots, r_{jH}\right] \end{aligned} \tag{17}$$

where

$$\begin{aligned} r_{j(n-1)} + d_c \le r_{in} \le r_{j(n+1)} - d_c \quad n = 1, 2, \ldots, H-1 \\ r_{i(n-1)} + d_c \le r_{jn} \le r_{i(n+1)} - d_c \quad n = 1, 2, \ldots, H-1 \end{aligned} \tag{18}$$

Mutation. If the mth gene of lth individuals is selected as mutation gene.

The premutation genetic operator is

$$\boldsymbol{R}_l = [r_{l0}, r_{l1}, r_{l2}, \ldots, r_{lm}, \ldots, r_{lH}] \tag{19}$$

The postmutation genetic operator is

$$\boldsymbol{R}_l' = [r_{l0}, r_{l1}, r_{l2}, \ldots, r_{lmu}, \ldots, r_{lH}] \tag{20}$$

where

$$r_{l(m-1)} + d_c < r_{lmu} < r_{l(m+1)} - d_c \quad m = 1, 2, \ldots H-1. \tag{21}$$

The individual, after performing the crossover and mutation, forms next generation population $\boldsymbol{P}_{\mathrm{g}}$.

$$\boldsymbol{P}_g = \left[\boldsymbol{R}_1', \boldsymbol{R}_2', \ldots, \boldsymbol{R}_k'\right] \tag{22}$$

4. Simulation

In order to verify the efficiency of proposed method, two simulations were performed. We set some common parameters

Table 3: Comparing the optimal result of $N = 201$ and $H = 7$ with [21, 22]. Function model algorithm using MGA (FMAMGA), element number (N), ring radii ($r_n(\lambda)$), and element number in the rings (N_n).

method	PSLL (dB)	N	n	1	2	3	4	5	6	7
HGA [21]	-22.94	201	$r_n(\lambda)$	1.0	1.59	2.14	2.88	3.66	4.98	--
			N_n	12	19	26	36	45	62	--
Opt r_n by MGA [22]	-25.45	201	$r_n(\lambda)$	0.80	1.38	1.88	2.43	3.18	3.91	4.98
			N_n	10	17	22	27	33	40	51
MGAFMA	-26.21	201	$r_n(\lambda)$	0.72	1.22	1.72	2.39	3.18	3.93	4.98
			N_n	9	15	21	28	35	41	51

Table 4: Comparing the optimal result of $N = 142$ and $H = 6$ with [21, 22]. Function model algorithm using MGA (FMAMGA), element number (N), ring radii ($r_n(\lambda)$), and element number in the rings (N_n).

method	PSLL (dB)	N	n	1	2	3	4	5	6
Opt r_n&N_n [21]	-27.82	142	$r_n(\lambda)$	0.76	1.36	2.09	2.99	3.78	4.70
			N_n	9	17	25	31	26	33
Opt r_n by MGA [22]	-28.07	142	$r_n(\lambda)$	0.76	1.36	2.09	2.92	3.77	4.70
			N_n	9	16	26	30	27	33
FMAMGA	-28.19	142	$r_n(\lambda)$	0.84	1.37	2.10	2.95	3.78	4.70
			N_n	10	17	25	29	29	31

for two simulations, such as selecting equation (4) as objective function and the minimum element spacing $d_c = \lambda/2$; the radiation pattern in the u-region ($-1 \le u \le 1$) and v-region ($-1 \le v \le 1$) is sampled 1024 points. The basic parameters of MGA are set as follows: the number of genetic generations is 200, the individual number of populations is 100, truncate rate is 50%, crossover rate is 20%, mutation rate is 2%, and elitism is also employed.

4.1. Optimizing Sparse Concentric Ring Arrays with the Number of Elements N = 201. We set the same parameter values as [21, 22]; that is, the number of elements $N = 201$, and the aperture $L = 9.96\lambda$. If ring number $H = 6$, the arrays are almost full and the element spacing is equal to nearly d_c; there is no room for optimization; thus let the number of rings $H = 7$. Set the coefficient of function model $a = -0.0072$, $b = 0.0036$, and $c = 0.6973$. Five independent experiments were carried out in this simulation, and convergence curve takes the average of 5 independent experiments. The radiation pattern, the element configuration diagram, and the cut surface of $u = 0$, $v = 0$ are from the optimal result of 5 experiments. The element configuration of the best sparse concentric ring array is shown in Figure 4. Figure 5 shows the radiation pattern of the optimal result. The cut surface of $u = 0$ and $v = 0$ is shown in Figure 6. The PSLL of optimal result is -26.21 dB, and it is lower 3.27 dB than [21] and lower 0.76 dB than [22]. Figure 7 shows the convergence characteristics of function model algorithm using MGA, and the proposed method has fast convergence characteristic. Contrast with that of [21, 22] is shown in Table 3.

4.2. Optimizing Sparse Concentric Ring Arrays with the Number of Elements N = 142. According to [21, 22], set the number of elements $N = 142$, the aperture $L = 9.4\lambda$, and the number

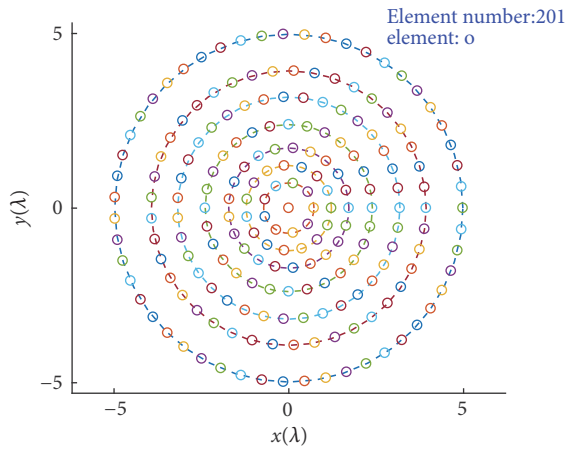

Figure 4: The diagram of element configuration.

of rings $H = 6$. Set the coefficient of function model $a = -0.1969$, $b = 0.00228$, and $c = 0.6543$. Five independent experiments were carried out in this simulation, and convergence curve takes the average of 5 independent experiments. The radiation pattern, the element configuration diagram, and the cut surface of $u = 0$, $v = 0$ are from the optimal result of 5 experiments. The element configuration of the best sparse concentric ring array is shown in Figure 8. Figure 9 shows the radiation pattern of the optimal result. The cut surface of radiation pattern when $u = 0$ and $v = 0$ is shown in Figure 10. The PSLL of optimal result is -28.19 dB, and it is lower 0.37 dB than [21] and lower 0.12 dB than [22]. Figure 11 shows the convergence characteristics function model algorithm using MGA, and the proposed method has fast convergence characteristic. Contrast with that of [21, 22] is shown in Table 4.

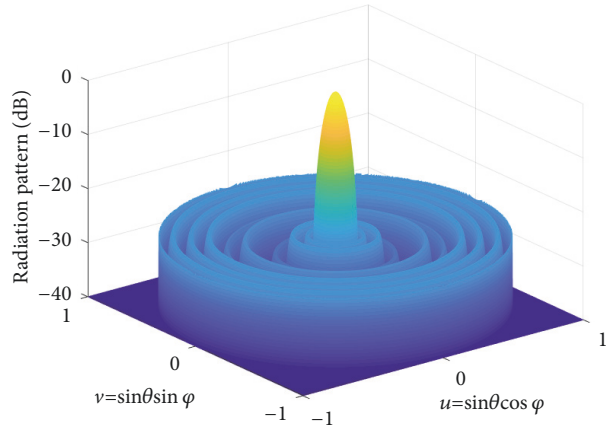

Figure 5: Radiation pattern of the optimal result.

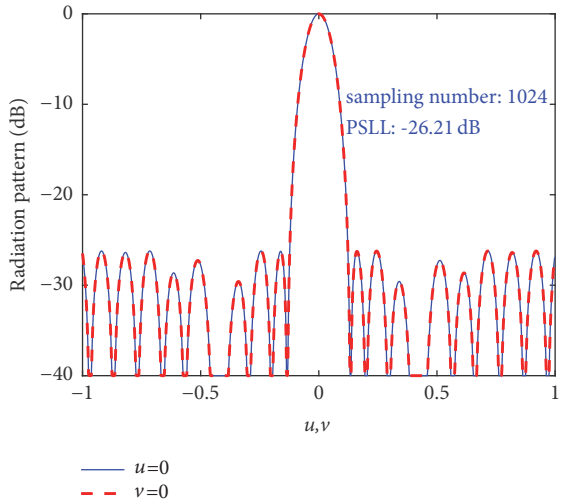

Figure 6: The cut of radiation pattern $u = 0$, $v = 0$.

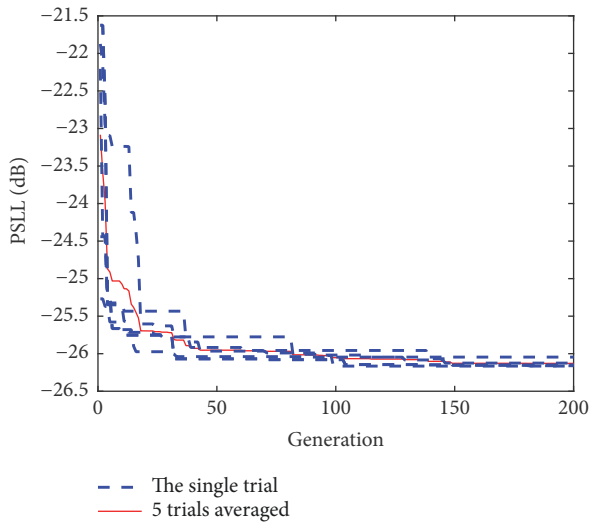

Figure 7: The convergence characteristics.

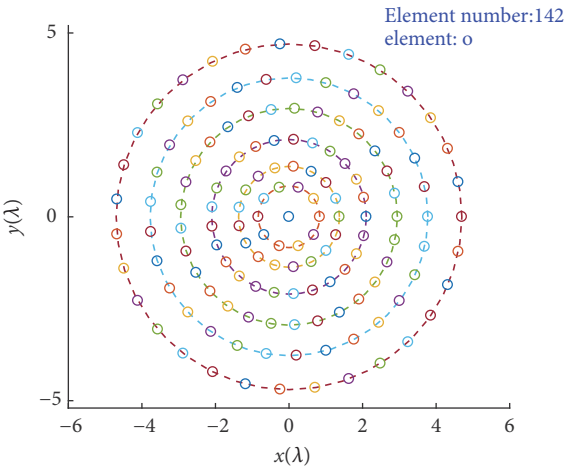

Figure 8: The diagram of element configuration.

5. Conclusion

In this paper, a function model that presents the relationship between ring radius and the degree of sparsity is proposed, which is embedded into the process of MGA to synthesize the sparse concentric ring arrays for low PSLL. Comparing the optimal result with other literatures proves that the proposed method is an efficient way to reduce the PSLL and has a faster convergence rate. It is reasonable and efficient to select the element number in the rings according to the function model.

Data Availability

The data of this paper can be accessed for the public; the data have been uploaded to github repository and all the data present in the research are available. The chart, docx data used to support the findings of this study, the result of figure, and the program of this research have been deposited to the

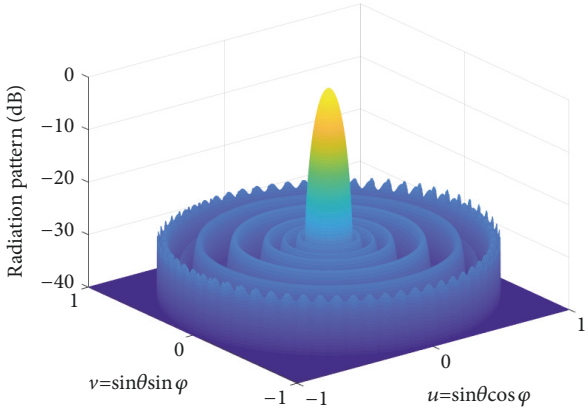

Figure 9: Radiation pattern of the optimal result.

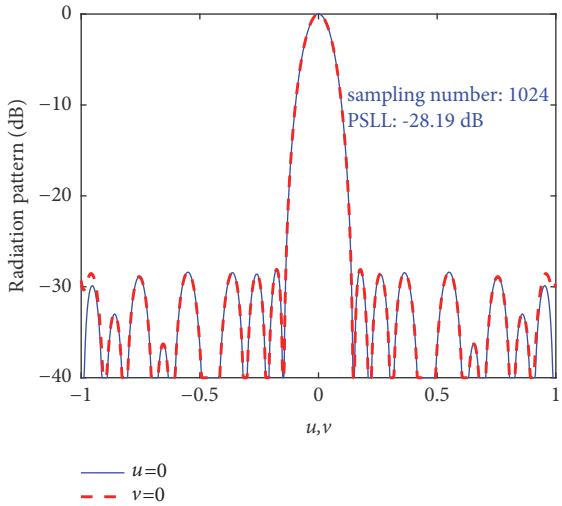

Figure 10: The cut of radiation pattern $u = 0$, $v = 0$.

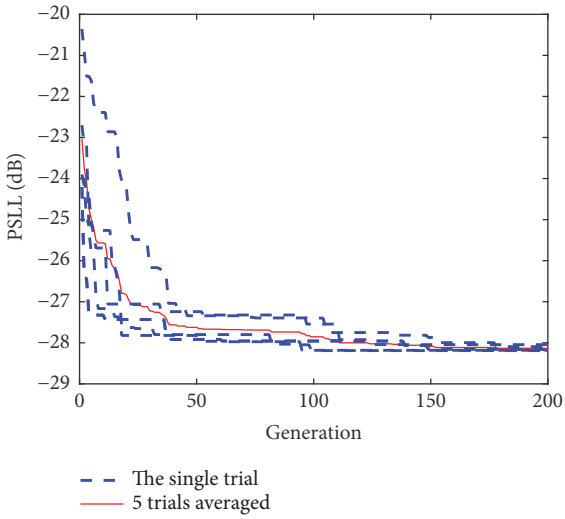

Figure 11: The convergence characteristics.

github repository; these data can be accessed through https://github.com/1367356/Optimization-of-sparse-concentric-ring-arrays-for-low-sidelobe.

Conflicts of Interest

Kesong Chen, Yafei Li, and Jiajia Shi declare that there are no conflicts of interest regarding the publication of this paper.

Acknowledgments

The research is funded by joint fund for civil aviation (U1233103).

References

[1] A. R. Maldonado, M. A. Panduro, C. Del Rio Bocio, and A. L. Mendez, "Design of concentric ring antenna array for a reconfigurable isoflux pattern," *Journal of Electromagnetic Waves and Applications*, vol. 27, no. 12, pp. 1483–1495, 2013.

[2] M. Ibarra, M. A. Panduro, Á. G. Andrade, and A. Reyna, "Design of sparse concentric rings array for LEO satellites," *Journal of Electromagnetic Waves and Applications*, vol. 29, no. 15, pp. 1983–2001, 2015.

[3] T. Jinpil, K. Kyeol, K. Sunwoo et al., "Dual-band on-body repeater antenna for in-on-on WBAN applications," *International Journal of Antennas and Propagation*, vol. 2013, Article ID 107251, 12 pages, 2013.

[4] W.-J. Zhang, L. Li, and F. Li, "Reducing the number of elements in linear and planar antenna arrays with sparseness constrained optimization," *IEEE Transactions on Antennas and Propagation*, vol. 59, no. 8, pp. 3106–3111, 2011.

[5] H. Steyskal, "The Woodward-Lawson method - To bury or not to bury?" *IEEE Antennas and Propagation Society Newsletter*, vol. 31, no. 1, pp. 35-36, 1989.

[6] P. Minvielle, E. Tantar, A.-A. Tantar, and P. Berisset, "Sparse antenna array optimization with the cross-entropy method," *IEEE Transactions on Antennas and Propagation*, vol. 59, no. 8, pp. 2862–2871, 2011.

[7] Q.-Q. He and B.-Z. Wang, "Design of microstrip array antenna by using active element pattern technique combining with taylor synthesis method," *Progress in Electromagnetics Research*, vol. 80, pp. 63–76, 2008.

[8] R. L. Haupt, "Thinned arrays using genetic algorithms," *IEEE Transactions on Antennas and Propagation*, vol. 42, no. 7, pp. 993–999, 1994.

[9] A. Trucco and V. Murino, "Stochastic optimization of linear sparse arrays," *IEEE Journal of Oceanic Engineering*, vol. 24, no. 3, pp. 291–299, 1999.

[10] D. G. Kurup, M. Himdi, and A. Rydberg, "Synthesis of uniform amplitude unequally spaced antenna arrays using the differential evolution algorithm," *IEEE Transactions on Antennas and Propagation*, vol. 51, no. 9, pp. 2210–2217, 2003.

[11] J. Robinson and Y. Rahmat-Samii, "Particle swarm optimization in electromagnetics," *IEEE Transactions on Antennas and Propagation*, vol. 52, no. 2, pp. 397–407, 2004.

[12] M. A. Panduro, A. L. Mendez, R. Dominguez, and G. Romero, "Design of non-uniform circular antenna arrays for side lobe reduction using the method of genetic algorithms," *AEÜ - International Journal of Electronics and Communications*, vol. 60, no. 10, pp. 713–717, 2006.

[13] M. A. Panduro and C. A. Brizuela, "Evolutionary multi-objective design of non-uniform circular phased arrays," *COMPEL: The International Journal for Computation and Mathematics in Electrical and Electronic Engineering*, vol. 27, no. 2, pp. 551–566, 2008.

[14] M. A. Panduro, C. A. Brizuela, J. Garza, S. Hinojosa, and A. Reyna, "A comparison of NSGA-II, DEMO, and EM-MOPSO for the multi-objective design of concentric rings antenna arrays," *Journal of Electromagnetic Waves and Applications*, vol. 27, no. 9, pp. 1100–1113, 2013.

[15] M. A. Panduro, C. A. Brizuela, and D. H. Covarrubias, "Design of electronically steerable linear arrays with evolutionary algorithms," *Applied Soft Computing*, vol. 8, no. 1, pp. 46–54, 2008.

[16] L. A. Garza, L. F. Yepes, D. H. Covarrubias, M. A. Alonso, and M. A. Panduro, "Synthesis of sparse circular antenna arrays applying a tapering technique over reconstructed continuous current distribution," *IET Microwaves, Antennas & Propagation*, vol. 10, no. 3, pp. 347–352, 2016.

[17] J. H. Holland, *Adaptation in Natural and Artificial System*, MIT Press, 1992.

[18] K. Chen, H. Chen, L. Wang et al., "Modified real GA for the synthesis of sparse planar circular arrays," *IEEE Antennas and Wireless Propagation Letters*, vol. 15, p. 1, 2016.

[19] R. Das, "Concentric ring array," *IEEE Transactions on Antennas and Propagation*, vol. 14, no. 3, pp. 398–400, 1966.

[20] R. L. Haupt, "Thinned concentric ring arrays," in *Proceedings of the Antennas and Propagation Society International Symposium*, 2008.

[21] R. L. Haupt, "Optimized element spacing for low sidelobe concentric ring array," *IEEE Transactions on Antennas and Propagation*, vol. 56, no. 1, pp. 266–268, 2008.

[22] C. Kesong, Z. Yongyun, and N. I. Xiaolong, "Optimum method of grid ring radii of sparse concentric rings array," *Chinese Journal of Radio Science*, 2016.